Studies on Risperidone Loaded β-Cyclodextrin Nanosponges for Managing Altered Mental Status and Delirium in Cancer Patients

Mohd Muqtader Ahmed[1,*], P. Ravi[1], K.E. Pravallika[1] and Sarwat Hazeeqa[2]

[1]*University College of Pharmaceutical Sciences, Acharya Nagarjuna University, Nagarjuna Nagar, Guntur Dt, AP-522510, India*

[2]*Hayatt Health Care & Azur Pharmaceuticals, Zaheerabad, Telangana- 502220, India*

Abstract: This study explores the prospective of risperidone-loaded β-cyclodextrin nanosponges as a therapeutic strategy for managing altered mental status (AMS) and delirium in cancer patients. Almost 87% of patients with advanced cancer experience AMS or delirium, significantly impacting prognosis and quality of life. The present study aims to enhance the solubility, bioavailability, and therapeutic effectiveness of second-generation antipsychotic medication risperidone (RSP), with poor aqueous solubility, it was encapsulated in β-cyclodextrin nanosponges. The nanosponges prepared by fusion technique using different β-CD: DPC molar ratios, were tested for their ability to encapsulation efficiency, drug loading, and dissolutions kinetics. Batch 1, (1:1 molar ratio) exhibits RSP loading capacity (454.2 µg/mg) and encapsulation efficiency (90.84%) along with DSC and FTIR also confirmed that the RSP was successfully encapsulated and without any chemical interactions. *In vitro* dissolution studies demonstrated a biphasic release profile, with an initial burst followed by sustained release, governed by Fickian diffusion as confirmed by release kinetics modeling. The improved solubility and dissolution profile of the nanosponges will be significant to improve risperidone delivery, ensuring better symptom management in a vulnerable population. These findings highlight the potential of β-cyclodextrin nanosponges as an innovative and adaptable platform for enhancing antipsychotic drug delivery.

Keywords: Altered Mental Status, β-Cyclodextrin Nanosponges, Cancer Patients, Delirium, Drug Delivery Systems, Risperidone.

INTRODUCTION

Globally, neuropsychiatric complications such as altered mental status (AMS) and delirium affect a significant proportion of patients. These conditions, characterized by cognitive dysfunction, confusion, and disorientation, impact approximately 40% of geriatric patients in emergency settings and up to 87% of cancer patients in advanced stages [1]. Another factors that may causes AMS and delirium are metabolic disturbances, brain metastases, narcotics interactions, and systemic inflammation, that significantly impacts the patient life. Despite their prevalence, up to 76% of delirium cases go undiagnosed due to fluctuating symptoms and diagnostic challenges. Management medications includes; risperidone, olanzapine and quetiapine [2]. Moreover, delirium indicates poorer prognosis, of which 50% of cases are reversible when triggers are well addressed [3].

Both mental disorders and cancer management reflects substantial clinical challenges and chances for exploration. Individuals suffering from neurological disorders such as delirium, schizophrenia, bipolar disorder, and acute mass seizures tend to have poor prognoses in cancer screening, delays in diagnosis, and low medication adherence to standard treatment protocols [4]. For example, less diagnostic screening, stigma, and healthcare access are some of the obstacles that patients with severe mental illnesses (SMIs) often encounter when trying to get a timely cancer diagnosis and medical treatment [5,6].

Furthermore, hallucinations and delusions are other psychotic symptoms that make it even more difficult to communicate with patients, get them to comply with their chemotherapeutics treatment plans, and manage them well as a whole [7,8].

Chou *et al*. (2016) explored the complex relationship between schizophrenia and cancer, people with schizophrenia have a 20% shorter life expectancy than the overall population. Schizophrenia affects 0.31–1% of the population [9]. Poor lifestyle habits, cognitive impairments, physician bias, and institutional stigma are often cited as causes of the incongruences in cancer care. These factors contribute to lower screening rates, longer treatment delays, and less access to effective therapies. Curiously, there is evidence that tumor-suppressor gene activity or the effects of antipsychotic drugs may be responsible for a reduced incidence of certain cancers in schizophrenia patients. But mortality rates are still high, mostly because people are diagnosed too late and don't get

*Address correspondence to this author at the University College of Pharmaceutical Sciences, Acharya Nagarjuna University, Nagarjuna Nagar, Guntur Dt, AP-522510, India; E-mail: mohdmuqtadarscholar@gmail.com

ISSN: 1929-2260 / E-ISSN: 1929-2279/24

enough treatment. Additionally, studies investigating the chemotherapeutic effects of antipsychotic medications need to be exploited [10].

Higher cancer mortality due to delayed diagnoses, suboptimal treatment, and stigma was emphasised by Grassi *et al.* (2023) in their analysis of cancer care disparities affecting individuals with severe mental illness [11].

Emerging evidence indicates that cancer and psychiatric disorders share complex biological interactions, involving immune dysregulation, heightened natural killer cell activity, tumor suppressor gene overexpression, systemic inflammation, and neuroinflammatory pathways, underscoring the need for integrated oncology and psychiatry care [9,12-14]. Antipsychotic medications like risperidone (RSP) are effective in managing neuropsychiatric symptoms in cancer patients, with remission achieved in up to 40% of delirium cases [15].

Drug selected for this study was RSP, soluble in organic solvents such as ethanol, poorly aqueous soluble, mol.wt (410.49 g/mol), and a pKa (8.7) [16]. It acts primarily by antagonizing dopamine D2 and serotonin 5-HT2A receptors, reducing positive symptoms and improving negative symptoms in schizophrenia while minimizing extrapyramidal side effects. Its sedative effects are related to its moderate activity at adrenergic and histamine H1 receptors. The drug is metabolized by CYP2D6 into 9-hydroxy-risperidone, readily excreted in urine, and has a half-life of 20hours. It is quickly absorbed and has a bioavailability of approximately 70% and a plasma protein binding affinity of around 90%. For the treatment of schizophrenia, bipolar mania, and autism-related irritability disorders, the recommended dosage is 2–5 mg per day for adults and 0.25–0.5 mg per day for children [17-19].

By addressing issues like low solubility and bioavailability, nano delivery systems like β-cyclodextrin nanosponges improve therapeutic efficacy through better dissolving and sustained release. [20,21]. Cancer care for people with mental illness is already complicated, and the psychosocial component just makes things worse. Combining pharmaceutical, psychological, and social interventions in novel patient-centered ways is necessary to address these systemic disparities [4,7,22].

The present study aims to enhance the solubility, bioavailability, and therapeutic effectiveness of poorly water soluble second-generation antipsychotic medication risperidone (RSP), by encapsulating it in β-cyclodextrin nanosponges.

MATERIALS AND METHODS

Materials

β-cyclodextrin (βCD), Diphenyl carbonate, Dimethyl sulfoxide (DMSO), Trimethylamine are procured from Sigma Aldrich, Germany. All the other solvents were used as procured without any processing.

Higuchi and Connors Solubility Studies

Calibration curve was constructed for 2.5 - 25 µg/mL by serially diluting a stock solution of 100 ppm (100 µg/mL) risperidone HPLC garde Methanol, drug concentration was then determined by HPLC (HPLC System, Waters, Illinois, USA) using UV detector at 284 nm. Phase solubility study was performed by adding RSP in excess amount to the β-CD solution prepared in water with final concentrations of 0.5 - 5 mM, suspension was then subjected to thermody-namically stable water bath mechanical shaker (Julabo SW23 Shaking Water Bath, Seelbach, Germany) adjusted at 25°C, 100 rpm for 72 hours [23]. The aliquots were then membrane filtered (0.45 µm filter) and analyzed for the drug absorbance at 284 nm [24-26]. Solubilized RSP concentrations were calculated using the calibration curve. The stability constant (Kc) was calculated using the equation:

$$K_c = \frac{slope}{1 - slope}$$

where the slope is derived from the phase solubility plot. Complexation Efficiency (CE) was also calculated to evaluate the efficiency of β-CD in forming inclusion complexes.

Preparation of β-CD Nanosponges

Four batches of 5gm each blank β-CD nanosponges were prepared by fusion technique wherein β-CD and cross linker diphenyl carbonate (DPC) in molar proportion (1:1,1:2,1:3 and 1:4) were prepared by melting them in porcelain dish at 90°C after formation of melted dispersion 0.5mL trimethylamine (Et_3N) was also added to accelerates β-CD crosslinking with DPC by catalyzing nucleophilic substitution reaction. Fused β-CD-DPC nanosponges may contains the residual phenol moieties which could be removed by washing with milli-Q water followed by

Table 1: Formulation and Characterization of β-CD Nanosponges

Batch	β-CD:DPC Molar Ratio	β-CD (g)	DPC (g)	Moles β-CD	Moles DPC	EE (%)	DLC (µg/mg)
Batch 1	01:01	4.55	0.45	0.00401	0.0021	90.84	454.2
Batch 2	01:02	4.03	0.97	0.00355	0.00455	85.64	428.2
Batch 3	01:03	3.53	1.47	0.00311	0.00687	70.56	352.8
Batch 4	01:04	3.06	1.94	0.0027	0.0091	67.54	337.7

extraction using organic solvent acetone. Prepared β-CD nanosponges then subjected to the hot-air oven at 40°C to remove the moisture and packed in glass vial for upcoming drug loading process [27].

RSP Loading in β-CD Nanosponges

Drug (RSP) was loaded in 1:1 ratios in all the four batches of prepared β-CD nanosponges, by solubilizing RSP in EtOH:DMSO(1:1;2mL) followed by dispersing it in the aqueous solution of β-CD nanosponges (3mL). the suspension was then ultrasonicated (2min). RSP loaded β-CD nanosponges was then kept on magnetic stirrer (100rpm) to evaporate the solvents. The samples then scrapped and sealed for further analysis.

Encapsulation Efficiency and Drug Loading Capacity

To assure optimal drug encapsulation and therapeutic efficiency, it is crucial to quantitatively analyze Encapsulation Efficiency (EE %) and Drug Loading Capacity (DLC) and to evaluate the efficacy of β-CD nanosponges in prepared batches. Drug-loaded nanosponges were dissolved in ethanol and analysed at 284 nm using HPLC (HPLC System, Waters, Illinois, USA) to determine the concentration of the encapsulated drug. DLC and RSP loading capacity EE (%) were used to calculate the encapsulation process's effectiveness. These computations highlights the efficacy of the drug-loading process and the nanosponges' applicability for drug delivery applications [24-26].

$$EE(\%) = \frac{Weight\ of\ RSP\ Encapsulated}{Initial\ Weight\ of\ RSP\ added} \times 100$$

$$DLC = \frac{Weight\ of\ RSP\ Encapsulated}{Total\ Weight\ of\ \beta CD\ Nanosponges + RSP}$$

The results of these calculations enlighten on how well the drug-loading technique and β-CD –DPC ratios worked and whether or not the nanosponges were appropriate for use as drug delivery vehicles.

Fourier-Transform Infrared Spectroscopy

FTIR was performed to analyze RSP, β-CD, RSP-loaded β-CD nanosponges, and their physical mixture. Each sample was finely powdered, mixed with KBr in gray agate mortar Pestle, filled to die and compressed by into thin pellets using a hydraulic press. The FTIR spectra (FTIR- Spectrophotometer, Jasco model 4700, Tokyo, Japan) were recorded in the range of 4000–400 cm^{-1}. The spectra were analyzed to detect characteristic peaks, shifts, or changes, providing insights into the interactions between RSP and β-CD in the nanosponges.

Differential Scanning Calorimetry

The thermal characteristics of RSP, β-CD, RSP-loaded β-CD nanosponges, and their physical mixture in approximate amount (5mg) were examined by Differential Scanning Calorimetry (DSC) (Scinco, model N-650, Seoul, Korea), samples were filled and crammed into a hemispherical aluminum pan. To avoid oxidation, samples were heated in a nitrogen environment from 40°C to 250°C at a rate of 10°C per minute. In order to identify thermal transitions such melting points, glass transitions, or breakdown, thermograms were recorded [28].

In-Vitro Dissolution and Release Kinetics

A USP-II apparatus (Erweka model DT 600, Heusnstamm, Germany), a rotating paddle at 50 rpm, PBS (pH 7.4) + 0.5 percent surfactant (SLS), and 37±0.5°C parameters were used for the dissolution study. Maintaining the sink condition after withdrawing 5mL sample at pre-determined time intervals, membrane filtered and analyzed as disused in the aforementioned EE method. Excel 2016 software used to calculate the cumulative % RSP released with respective to time, release profiles plotted, for RSP-Pure, RSP- β-CD and β-CD nanosponges (batch1) containing equivalent 10mg RSP. The dissolution data further processed for the release kinetics to determine the mechanism of release by fitting the data in four kinetic model as showed in the Table **2** [29].

Mean Dissolution Time & Dissolution Efficiency

The Mean Dissolution Time (MDT) and Dissolution Efficiency (DE) were calculated by;

$$MDT = \frac{\sum (t_i . \Delta M_i)}{\sum \Delta M_i}$$

$$DE = \frac{\int_0^t y(t)dt}{y_{100} . t} \times 100$$

The midpoints of the time intervals were calculated as the average of successive time points, and the incremental drug release (ΔM_i) was determined as the difference in %CDR between successive time points. The weighted sum of the midpoints ($t_i \cdot \Delta M_i$) was divided by the total incremental drug release ($\Sigma \Delta M_i$) to calculate MDT.

DE is a significant parameter as it reflects the overall release efficiency, integrating both rapid and sustained phases of drug release. A high DE value indicates effective drug dissolution and highlights the suitability of the delivery system for therapeutic applications [30].

RESULT

Higuchi and Connors Solubility Studies

According to the Higuchi and Connors classification method, the phase solubility profile indicated an AL-type profile, with RSP solubility increasing linearly with increasing β-CD proportions. The baseline solubility of RSP in the absence of β-CD was 4.36 µg/mL. The solubility increased dramatically with increasing β-CD concentrations, peaking at 20.14 µg/mL at 2 mM β-CD, which is 4.6 times higher than baseline. The solubility plateaued after 2 mM, most likely as a result of the β-CD cavity becoming saturated. A computed stability constant (Kc) of 147.2 M^{-1}, indicating a moderate binding strength, was obtained from the phase solubility plot with a slope of 0.032. With complexation efficiency (CE) values ranging from 0.065 to 0.206, the effectiveness of β-CD in solubilizing RSP was confirmed. With β-CD, RSP's solubility increases linearly, maximum peak values that indicated binding strength. Similar patterns were noted with methylated β-CDs, which Sbarcea *et al.* [31] found further improved solubility.

Preparation of β-CD Nanosponges

The fusion technique was used to successfully prepare four batches of β-CD nanosponges with different molar ratios of β-CD to diphenyl carbonate (DPC) Table **1**. Batch 1 had a ratio of 1:1, 4.55 g β-CD and 0.45 g DPC; Batch 2 had a ratio of 1:2, 4.03 g β-CD and 0.97 g DPC; Batch 3 had a ratio of 1:3, 3.53 g β-CD and 1.47 g DPC; and Batch 4 had a ratio of 1:4, 3.06 g β-CD and 1.94 g DPC. To ensure efficient crosslinking, trimethylamine (Et3N), a catalyst for the nucleophilic substitution process, was added. To remove any last traces of phenol moieties, we soxhlet extraction with acetone was done followed by Milli-Q water washing. The nanosponges were then dried at 40°C to make sure they were free from moisture and water traces before being stored in sealed jars.

RSP Loading in β-CD Nanosponges

RSP loading process into the β-CD nanosponges by first solubilizing it in a solvent system (EtOH:DMSO), followed by ultrasonication enabled the

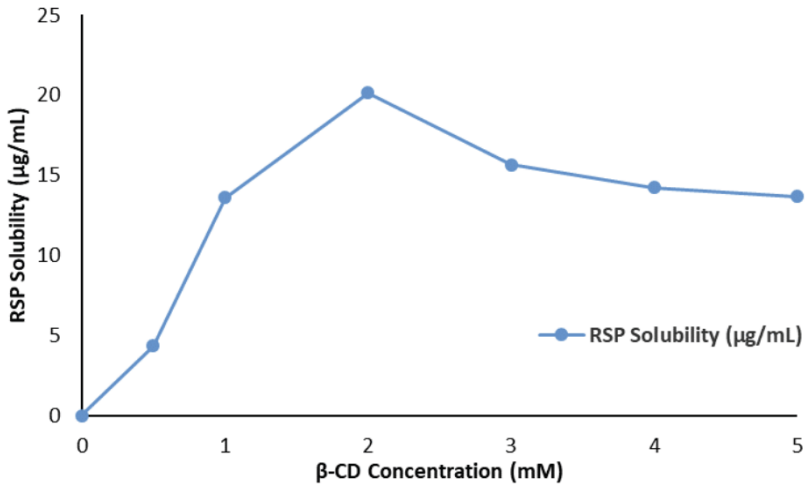

Figure 1: Effect of β-CD Concentration on RSP Solubility.

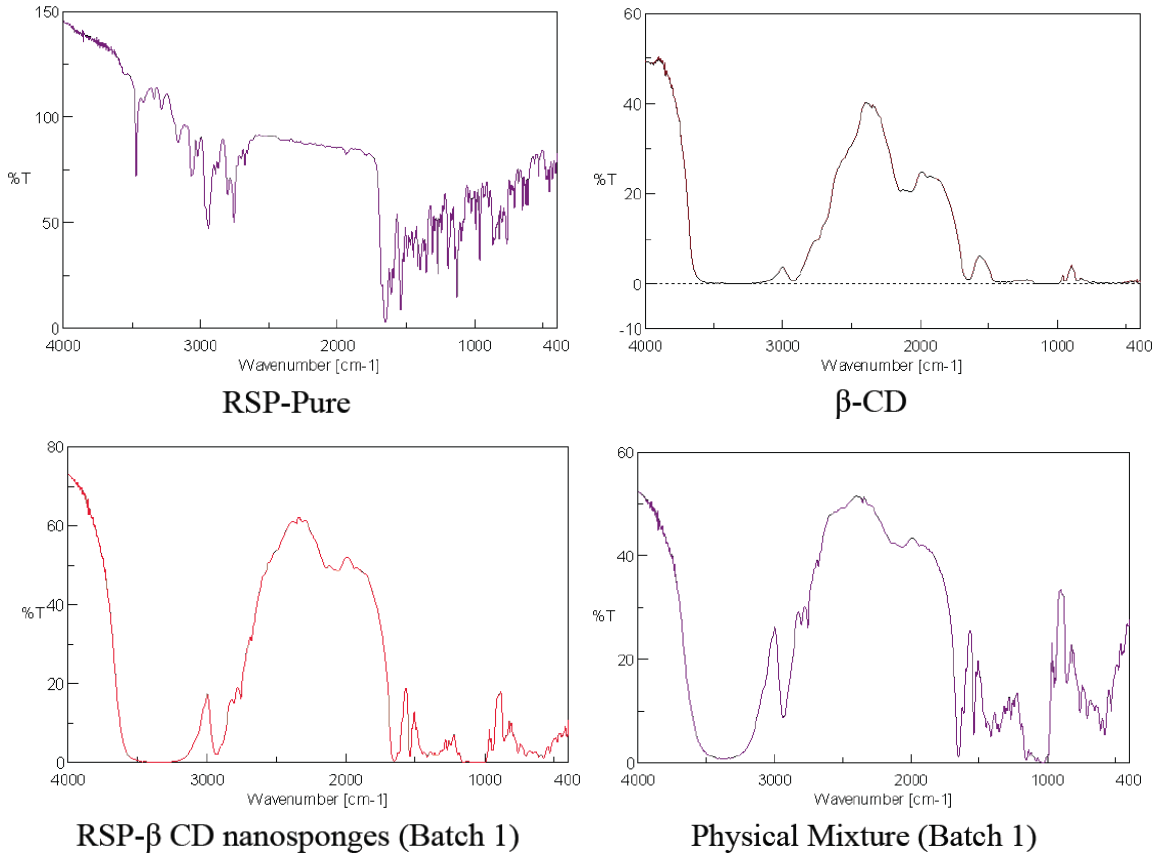

Figure 2: FTIR Spectra of RSP, β-CD, Nanosponges, and Physical Mixture.

drug to interact with the nanosponge cavities. The encapsulation was solidified by aiding solvent evaporation through magnetic stirring.

Encapsulation Efficiency and Drug Loading Capacity

EE represents the proportion of RSP within the β-CD nanosponges. Batch 1 exhibited the highest EE% (90.84%), followed by Batch 2 with 85.64%, Batch 3 with 70.56%, and Batch 4 with 67.54%, highlighting the impact of increasing cross linker decreasing RSP encapsulation. Similarly, Drug Loading Capacity (DLC), which quantifies the amount of RSP encapsulated per milligram of nanosponges, was highest in Batch 1 (454.2 µg/mg) and progressively decreased to Batch 4 (337.7 µg/mg). These results (Table **1**) demonstrate that lower crosslinking densities enhance both EE% and DLC, offering better encapsulation efficiency and drug loading capacity.

Fourier-Transform Infrared Spectroscopy

The FTIR spectrum of pure RSP showed characteristic peaks, including C=O stretching vibrations around 1650–1700 cm^{-1}, NH bending near 3300–3400 cm^{-1}, and aromatic C=C stretching at 1500–1600 cm^{-1}. β-CD exhibited distinct peaks, such as O-H stretching at 3300 cm^{-1}, C-H stretching at 2900 cm^{-1}, and C-O-C vibrations near 1150–1200 cm^{-1}. In RSP-β-CD nanosponges (Batch 1), shifts in the C=O stretching and reduced O-H stretching intensity confirmed hydrogen bonding and encapsulation of RSP within β-CD cavities, with the disappearance of some RSP peaks further supporting inclusion complex formation. The absence of chemical interactions was confirmed by the RSP-β-CD physical mixture, which displayed a straightforward superimposition of RSP and β-CD spectra.

Differential Scanning Calorimetry

The Differential Scanning Calorimetry (DSC) thermograms of pure risperidone (RSP), β-CD, RSP-loaded β-CD nanosponges (Batch 1), and the physical mixture of RSP and β-CD revealed significant differences. The crystalline nature of pure RSP was indicated by a sharp endothermic peak at about 176°C, whereas a broad endothermic peak about 110–130°C for β-CD. In RSP-loaded β-CD nanosponges, the sharp melting peak of RSP was absent, indicating successful encapsulation, along with a broadening and shift in the β-CD peak, suggesting interactions between RSP and

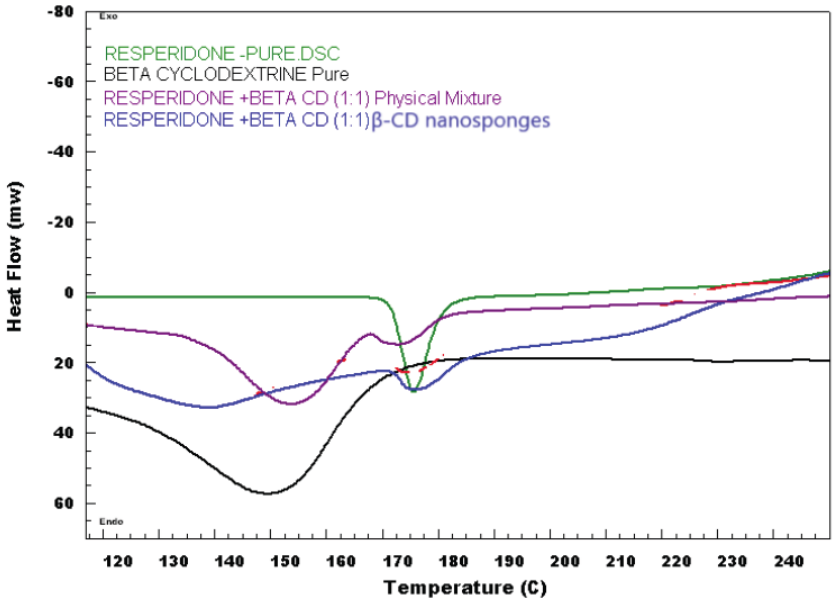

Figure 3: Thermograms of RSP, β-CD, Nanosponges, and Physical Mixture.

β-CD. In contrast, the physical mixture showed overlapping peaks of RSP and β-CD with presence of RSP peak, confirming the low drug encapsulation.

In-Vitro Dissolution and Release Kinetics

The *in-vitro* dissolution study of β-CD nanosponges revealed a biphasic drug release profile over 120 minutes. An initial burst release was observed, with over 75% of the drug released within the first 30 minutes (75.73 ± 6.39), followed by 100% release at the end of the study (100 ± 3.99). This release behavior suggests the rapid diffusion of surface-bound RSP molecules during the initial phase, followed by a sustained release from the nanosponges' matrix. These findings highlight the superior performance of β-CD nanosponges in enhancing drug release efficiency. In comparison, RSP Pure exhibited a much slower release of only 25.5% at 120 minutes (25.55 ± 0.61), while the Physical Mixture (PM) achieved 70.6% drug release (70.59 ± 8.03) over the same duration, Figure **4**.

Moreover, the dissolution data of β-CD nanosponges was fitted to various release kinetics models. The First-Order model provided the best fit, with an R^2 (0.976) followed by the Korsmeyer-Peppas model (0.952) and the Higuchi model (0.931). The Zero-Order model showed the least fit with an R^2 (0.724). The n-value obtained from the Korsmeyer-Peppas model was 0.401, indicating Fickian diffusion.

Mean Dissolution Time & Dissolution Efficiency

An average of 25.09 minutes was determined to be the Mean Dissolved Time (MDT), which indicates how

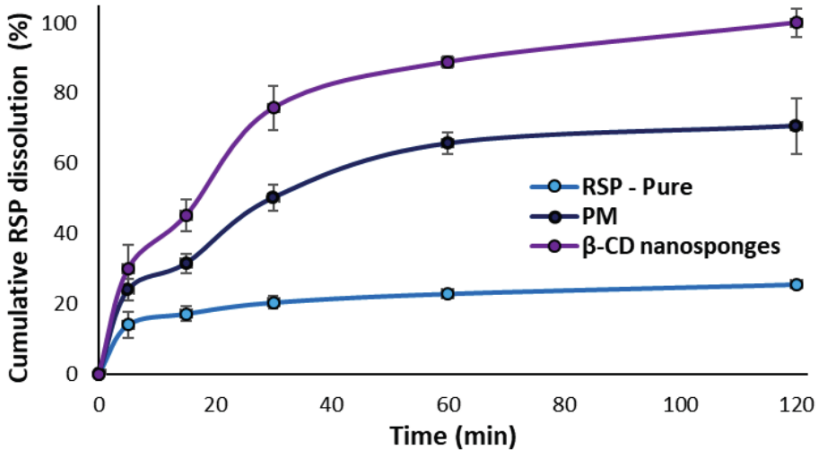

Figure 4: Dissolution Profiles of RSP Pure, PM, and β-CD Nanosponges.

Table 2: Release Kinetics Models and R^2 Coefficient

Kinetics Model	Equation	R^2 Value
Zero-Order	C = k0xt	0.724
First-Order	log(C) = log(k1) - k1xt	0.976
Higuchi	C = kH x sqrt(t)	0.931
Korsmeyer-Peppas	log(C) = log(k) + n x log(t)	0.952

long it takes for the drug to dissolve completely. The controlled release characteristics of the delivery system and the efficacy of the dissolving process were demonstrated by the determination of a Dissolution Efficiency (DE) of 78.5% over the 120-minute duration.

DISCUSSION

Higuchi and Connors Solubility Studies

The results confirm the formation of a 1:1 inclusion complex between RSP and β-CD, as reflected by the Addition, Linear (AL) type phase solubility profile. The significant enhancement in solubility, particularly the 4.6-fold increase, revealed the ability of β-CD to encapsulate the hydrophobic RSP, thereby improving its aqueous solubility. The stability constant **(**Kc**)** of 147.2 M^{-1} is within the optimal range for pharmaceutical applications, ensuring sufficient stability for complex formation while facilitating drug release. At higher β-CD concentrations, the solubility plateau indicates a saturation effect, which is typical in inclusion complex systems. These results show that β-CD can be used as a solubilizing agent, providing a viable method for increasing the bioavailability of RSP and other medications that are poorly soluble.

Preparation of β-CD Nanosponges

The crosslinking efficiency and structural properties of the β-CD nanosponges were greatly affected by the molar ratios of β -CD to DPC. Encapsulating larger or hydrophobic drug molecules became much easier with less dense crosslinking produced by lower ratios (Batch 1, 1:1), which allowed for more flexible cavities. On the other hand, denser cross-linked matrixes were produced by higher ratios (Batch 4, 1:4), which reduced cavity flexibility but may have improved stability for applications involving prolonged drug release. As a catalyst, trimethylamine was vital in hastening the nucleophilic substitution reaction and guaranteeing consistent β-CD nanosponges formation.

RSP Loading in β-CD Nanosponges

The β-CD nanosponges that are loaded with RSP show promise in enhancing the bioavailability and solubility of hydrophobic medications. Ideal for high solubilizations of medication and stability due to its superior encapsulation efficiency.

Encapsulation Efficiency and Drug Loading Capacity

Batch 1, with a β-CD:DPC molar ratio of 1:1, exhibited the highest EE of 90.84% and DLC of 454.2 µg/mg, reflecting efficient drug encapsulation due to the flexible and accessible β-CD cavities. In contrast, Batch 4 (1:4 molar ratio) showed the lowest EE 67.54% and DLC 337.7 µg/mg, attributed to increased rigidity and reduced cavity availability caused by higher crosslinking density. Lower crosslinking densities, as seen in Batch 1, favor encapsulation for applications requiring rapid drug release and high drug content, while higher crosslinking densities, as in Batch 4, provide structural stability for prolonged drug release. These promising of β-CD nanosponges as a versatile platform for encapsulating hydrophobic drugs like risperidone (RSP), with customization achievable by adjusting the β-CD:DPC molar ratio to suit specific therapeutic applications.

Fourier-Transform Infrared Spectroscopy

The RSP-β-CD nanosponges (Batch 1) and the physical mixture show clear spectral differences in the FTIR analysis. The achievement of RSP encapsulation within β-CD, leading to the formation of an inclusion complex, is validated by the noted peak shifts and intensity reductions in the nanosponges, RSP and β -CD cavities interact, and these changes, especially in the C=O and O-H regions, show strong hydrogen bonding. The absence of these spectral changes in the physical mixture, on the other hand, suggests that no interaction took place independent of the formation of nanosponges. This provides more evidence that prepared Batch 1 nanosponges can effectively

encapsulate RSP, and supports its functionality for enhancing RSP's solubility.

Differential Scanning Calorimetry

It is evident from the DSC thermograms that the RSP is enclosed within the β-CD nanosponges. The presence of RSP in the nanosponges matrix, most likely as a result of interactions at the molecular level, is confirmed by the fact that the thermograms of RSP-loaded β-CD nanosponges (Batch 1) does not show the sharp melting peak of RSP. The presence of hydrogen bonding or other forces between RSP and β-CD is further supported by the broadening and shift of the β-CD peak, which suggests these interactions. The lack of encapsulation or interaction was confirmed by the fact that the physical mixture maintained the characteristic peaks of both components. These results demonstrate that the β-CD nanosponge preparation method successfully encapsulates RSP and increases its stability, which could be useful in drug delivery systems.

In-Vitro Dissolution and Release Kinetics

Release mechanism of RSP from β-CD nanosponges was found to be diffusion, supported by the First-Order model, which strongly suggests a concentration-dependent mechanism, and by the Higuchi and Korsmeyer-Peppas models, the latter of which confirms Fickian diffusion due to the n-value (0.401). The results also emphasize, use of β-CD nanosponges for sustained drug delivery, with the capability to achieve biphasic release comprising both rapid and prolonged phases. This approach could have clinical significance by maintaining drug release within the therapeutic window. Consequently, the developed drug delivery systems may prove effective in managing AMS and delirium in patients with neurological challenges.

Mean Dissolution Time & Dissolution Efficiency

Both the short MDT and the high DE value indicate that the prepared drug delivery system can deliver a therapeutic dose within short time, and that the sustained release phase is very efficient. In the first burst release phase, the quick onset of action is guaranteed by the surface-bound drug molecules rapidly diffusing through the medium. On the other hand, the sustained release phase ensures that the drug remains available for a longer period of time by controlling the slow diffusion of the drug through the nanosponges' nanostructure. The suitability of β-CD nanosponges for both immediate and sustained drug delivery is further highlighted by their DE value of 78.5%, which further strengthens their dissolution efficiency.

CONCLUSION

Risperidone-loaded β-cyclodextrin nanosponges show promise in improving medication solubility, and dissolution could be beneficial for both AMS and delirium in cancer patients. The high encapsulation efficiency, drug-loading capacity, and enhanced dissolution features of the nanosponges improve patient adherence and symptom management. The nanosponge-based delivery system tackles risperidone administration problems by enabling improved medication release, making it a unique and effective alternative for susceptible and underserved patients. Future studies should explore clinical applications to validate these findings and further optimize this delivery system for broader therapeutic use including cancer therapy.

FUNDING STATEMENT

This research received no specific grant from any funding agency in the public, commercial, or not-for-profit sectors.

AUTHOR'S CONTRIBUTION

The manuscript was reviewed by P. Ravi, Analytical work supervised by K.E. Pravallika, Literature, data collection done by Hazeeqa Sarwat. The study was performed and manuscript written by Mohd Muqtader Ahmed.

REFERENCES

[1] LaHue SC, Douglas VC. Approach to altered mental status and inpatient delirium. Neurol Clin 2022; 40(1): 45-57. https://doi.org/10.1016/j.ncl.2021.08.004

[2] El Majzoub I, Abunafeesa H, Cheaito R, Cheaito MA, Elsayem AF. Management of altered mental status and delirium in cancer patients. Ann Palliat Med 2019; 8(5). https://doi.org/10.21037/apm.2019.09.14

[3] Bush SH, Tierney S, Lawlor PG. Clinical assessment and management of delirium in the palliative care setting. Drugs 2017; 77(15): 1623-1643. https://doi.org/10.1007/s40265-017-0804-3

[4] Bellman V, Russell N, Depala K, Dellenbaugh A, Desai S, Vadukapuram R, Patel S, Srinivas S. Challenges in treating cancer patients with unstable psychiatric disorder. World J Oncol 2021; 12(5): 137-148. https://doi.org/10.14740/wjon1402

[5] Bourgeois A, Horrill T, Mollison A, Stringer E, Lambert LK, Stajduhar K. Barriers to cancer treatment for people experiencing socioeconomic disadvantage in high-income countries: a scoping review. BMC Health Serv Res 2024; 24: 670. https://doi.org/10.1186/s12913-024-11129-2

[6] Weinstein LC, Stefancic A, Cunningham AT, Hurley KE, Cabassa LJ, Wender RC. Cancer screening, prevention, and treatment in people with mental illness. CA Cancer J Clin 2016; 66(2): 134-151. https://doi.org/10.3322/caac.21334

[7] Venkataramu VN, Ghotra HK, Chaturvedi SK. Management of psychiatric disorders in patients with cancer. Indian J Psychiatry 2022; 64(Suppl 2): S458-S472. https://doi.org/10.4103/indianjpsychiatry.indianjpsychiatry_15_22

[8] Kishi Y, Kato M, Okuyama T, Thurber S. Treatment of delirium with risperidone in cancer patients. Psychiatry Clin Neurosci 2012; 66(5): 411-417. https://doi.org/10.1111/j.1440-1819.2012.02346.x

[9] Chou FH, Tsai KY, Wu HC, Shen SP. Cancer in patients with schizophrenia: What is the next step? Psychiatry Clin Neurosci 2016; 70(11): 473-488. https://doi.org/10.1111/pcn.12420

[10] Oystacher T, Blasco D, He E, Huang D, Schear R, McGoldrick D, Link B, Yang LH. Understanding stigma as a barrier to accessing cancer treatment in South Africa: implications for public health campaigns. Pan Afr Med J 2018; 29: 73. https://doi.org/10.11604/pamj.2018.29.73.14399

[11] Grassi L, Riba MB. Disparities and inequalities in cancer care and outcomes in patients with severe mental illness: Call to action. Psychooncology 2021; 30(12): 1997-2001. https://doi.org/10.1002/pon.5853

[12] Zhang X, Ma L. Antipsychotics and tumor suppressor gene activity in cancer patients with schizophrenia. Transl Psychiatry 2013; 3: e288.

[13] Zhao H, Wu L, Yan G, Chen Y, Zhou M, Wu Y, Li Y. Inflammation and tumor progression: signaling pathways and targeted intervention. Signal Transduct Target Ther 2021; 6(1): 263. https://doi.org/10.1038/s41392-021-00658-5

[14] Eslami M, Memarsadeghi O, Davarpanah A, Arti A, Nayernia K, Behnam B. Overcoming chemotherapy resistance in metastatic cancer: a comprehensive review. Biomedicines 2024; 12(1): 183. https://doi.org/10.3390/biomedicines12010183

[15] Watkins CC, Sawa A, Pomper MG. Glia and immune cell signaling in bipolar disorder: insights from neuropharmacology and molecular imaging to clinical application. Transl Psychiatry 2014; 4(1): e350. https://doi.org/10.1038/tp.2013.119

[16] Rathi R, Mehetre NM, Goyal S, Singh I, Huanbutta K, Sangnim T. Advanced drug delivery technologies for enhancing bioavailability and efficacy of risperidone. Int J Nanomedicine 2024; 19: 12871-12887. https://doi.org/10.2147/IJN.S492684

[17] Alvarez-Herrera S, Rosel Vales M, Pérez-Sánchez G, Becerril-Villanueva E, Flores-Medina Y, Maldonado-García JL, Saracco-Alvarez R, Escamilla R, Pavón L. Risperidone decreases expression of serotonin receptor-2A (5-HT2A) and serotonin transporter (SERT) but not dopamine receptors and dopamine transporter (DAT) in PBMCs from patients with schizophrenia. Pharmaceuticals 2024; 17(2): 167. https://doi.org/10.3390/ph17020167

[18] Moran-Gates T, Grady C, Shik Park Y, Baldessarini RJ, Tarazi FI. Effects of risperidone on dopamine receptor subtypes in developing rat brain. Eur Neuropsychopharmacol 2007; 17(6-7): 448-55. https://doi.org/10.1016/j.euroneuro.2006.10.004

[19] Schotte A, Janssen PF, Gommeren W, Luyten WH, Van Gompel P, Lesage AS, De Loore K, Leysen JE. Risperidone compared with new and reference antipsychotic drugs: *in vitro* and *in vivo* receptor binding. Psychopharmacology 1996; 124(1-2): 57-73. https://doi.org/10.1007/BF02245606

[20] Pyrak B, Rogacka-Pyrak K, Gubica T, Szeleszczuk Ł. Exploring cyclodextrin-based nanosponges as drug delivery systems: understanding the physicochemical factors influencing drug loading and release kinetics. Int J Mol Sci 2024; 25(6): 3527. https://doi.org/10.3390/ijms25063527

[21] Koppula S, Maddi S. Nanosponges in therapeutics: Current advancements and future directions in targeted drug delivery. J Drug Deliv Sci Technol 2024; 101(Pt B): 106258. https://doi.org/10.1016/j.jddst.2024.106258

[22] Llave K, Cheng KK, Ko A, Pham A, Ericson M, Campos B, Perez-Gilbe HR, Kim JHJ. Promising directions: a systematic review of psychosocial and behavioral interventions with cultural incorporation for advanced and metastatic cancer. Int J Behav Med 2024; 31: 848-870. https://doi.org/10.1007/s12529-024-10264-8

[23] Saokham P, Muankaew C, Jansook P, Loftsson T. Solubility of cyclodextrins and drug/cyclodextrin complexes. Molecules 2018; 23(5): 1161. https://doi.org/10.3390/molecules23051161

[24] Rojek B, Bartyzel A, Sawicki W, Plenis A. DSC, TGA-FTIR and FTIR assisted by chemometric factor analysis and PXRD in assessing the incompatibility of the antiviral drug arbidol hydrochloride with pharmaceutical excipients. Molecules 2024; 29(1): 264. https://doi.org/10.3390/molecules29010264

[25] Mennickent S, de Diego M, Liser B, Trujillo L. Stability indicating HPLC method for quantification of risperidone in tablets. J Chil Chem Soc 2018; 63(3): 4150. https://doi.org/10.4067/s0717-97072018000304150

[26] Dedania ZR, Dedania RR, Sheth NR, Patel JB, Patel B. Stability indicating HPLC determination of risperidone in bulk drug and pharmaceutical formulations. Int J Anal Chem 2011; 2011: 124917. https://doi.org/10.1155/2011/124917

[27] Kumar S, Sihag P, Trotta F, Rao R. Encapsulation of Babchi oil in cyclodextrin-based nanosponges: physicochemical characterization, photodegradation, and *in vitro* cytotoxicity studies. Pharmaceutics 2018; 10(4): 169. https://doi.org/10.3390/pharmaceutics10040169

[28] Sbârcea L, Tănase IM, Ledeți A, Cîrcioban D, Vlase G, Barvinschi P, Miclău M, Văruţ RM, Suciu O, Ledeți I. Risperidone/Randomly Methylated β-Cyclodextrin Inclusion Complex-Compatibility Study with Pharmaceutical Excipients. Molecules 2021; 26(6): 1690. https://doi.org/10.3390/molecules26061690

[29] Alkilani AZ, Omar S, Nasereddin J, Hamed R, Obaidat R. Design of colon-targeted drug delivery of dexamethasone: Formulation and *in vitro* characterization of solid dispersions. Heliyon 2024; 10(14): e34212. https://doi.org/10.1016/j.heliyon.2024.e34212

[30] Mekasha YT, Wondie Mekonen A, Nigussie S, *et al*. Modeling and comparison of dissolution profiles for different brands of albendazole boluses. BMC Pharmacol Toxicol 2024; 25: 48. https://doi.org/10.1186/s40360-024-00774-2

[31] Sbârcea L, Tănase IM, Ledeți A, Cîrcioban D, Vlase G, Barvinschi P, Miclău M, Văruţ RM, Trandafirescu C, Ledeți I. Encapsulation of Risperidone by Methylated β-Cyclodextrins: Physicochemical and Molecular Modeling Studies. Molecules 2020; 25(23): 5694. https://doi.org/10.3390/molecules25235694

Received on 24-10-2024 Accepted on 20-11-2024 Published on 25-12-2024

https://doi.org/10.30683/1929-2279.2024.13.09